
Proceedings Paper:
Han, Y orcid.org/0000-0003-2141-3077, Partington, J, Chhantyal-Pun, R et al. (14 more authors) (2019) Broadband terahertz gas spectroscopy through multimode self-mixing in a quantum cascade laser. In: Razeghi, M, Baranov, AN and Vitiello, MS, (eds.) Proceedings of SPIE. SPIE Optical Engineering + Applications 2019: Terahertz Emitters, Receivers, and Applications X, 11-15 Aug 2019, San Diego, Calif., USA. SPIE . ISBN 9781510629417

https://doi.org/10.1117/12.2528683

Broadband terahertz gas spectroscopy through multimode self-mixing in a quantum cascade laser

Y. J. Han*[a], J. Partington[a], R. Chhantyal-Pun[a], E. Nuttall[a], M. Henry[b], O. Auriacombe[b], T. Rawlings[b], L. H. Li[a], J. Keeley[a], M. Oldfield[b], N. Brewster[b], R. Dong[a], P. Dean[a], A. G. Davies[a], B. N. Ellison[b], E. H. Linfield[a], A. Valavanis[a]
[a]School of Electronic and Electrical Engineering, University of Leeds, Leeds LS2 9JT, UK;
[b]Rutherford Appleton Laboratory, STFC, Harwell Oxford, Didcot OX11 0QX, UK

ABSTRACT

We present a self-mixing terahertz-frequency gas spectroscopy technique using a multimode quantum cascade laser. A precision-micro-machined external waveguide module and a double-metal quantum cascade laser device are used increase the optical feedback and the laser's frequency tuning range. Methanol spectra are measured using two laser modes at 3.362 THz and 3.428 THz simultaneously, with more than 8 absorption peaks resolved over a 17-GHz bandwidth, which provide minimum detectable absorption coefficients of 2.7×10^{-4} cm^{-1} and 4.9×10^{-4} cm^{-1}, respectively. In contrast to all previous self-mixing spectroscopy, our multimode technique expands the sensing bandwidth significantly. This broadband spectroscopy technique can potentially be used for the identification and analysis of chemical, biological radiological and nuclear (CBRN) agents and explosives.

Keywords: terahertz, quantum cascade laser, self-mixing, gas spectroscopy

1. INTRODUCTION

Chemical, biological radiological and nuclear (CBRN) agents and explosives have unique spectral signatures in the terahertz (THz) frequency range, which can be used for their identification and analysis[1-3]. Quantum cascade lasers (QCLs) are important sources within the 2–5 THz range[4-6], with merits including their compact size, coherence, narrow linewidth, tunable emission frequency, and high output power[7-10]. Heterodyne radiometry and direct-transmission gas spectroscopy have been demonstrated using THz QCLs[11-14], with their resolution and detectivity improved by phase locking, frequency modulation, and photoacoustic techniques[15-18]. These spectroscopy schemes have, until recently, required a separate detector or mixer as well as frequency calibration instrumentation, which increase the complexity and cost of the system. In order to overcome these challenges, a THz gas spectroscopy technique based on self-mixing (SM) in a QCL has been demonstrated[19]. SM interference occurs between the internal and backscattered optical fields in a laser cavity. This induces changes to the terminal voltage, which are sensitive to the amplitude and phase of the reflected radiation, thus enabling the laser device to act both as a radiation source and as a coherent detector[20, 21]. This technique removes the need for additional detectors and enables fast detection and self-calibration[22, 23]. However, the spectral bandwidth of these SM spectroscopy systems has so far been limited by the < 2 GHz tuning range of the single-mode QCLs used in previous works.

Here, we present the fabrication of THz frequency quantum cascade lasers (QCLs) emitting at 3.5 THz and a new and robust waveguide integration scheme. Based on the waveguide integrated QCL device, we also present a new technique, which exploits the ability of SM systems to monitor the full emission spectrum of their own laser source, and demonstrate the measurement of methanol spectral features simultaneously from two modes of a multi-mode THz QCL over a 17 GHz range.

2. DEVICE PROCESS

The active-region of the QCL used in this work is based on a GaAs/$Al_{0.15}Ga_{0.85}As$ phonon-enhanced bound-to-continuum design, which was grown using molecular beam epitaxy. The layer sequence of an active module in nanometers is

*y.han@leeds.ac.uk

3.7/10.5/**0.5**/12.2/**1**/12.5/**1.9**/11/**2.8**/8.8/**2.8**/7.9/**2.8**/6.6/**2.8**/15.8/**2.8**/13.8, where the $Al_{0.15}Ga_{0.85}As$ barriers are shown in bold and the doping density in the underlined GaAs well is 3.4×10^{16} cm^{-3}. The QCL device was processed into a double-metal (DM) ridge-waveguide structure. Ti/Au of thickness 10/500 nm was deposited on top of the QCL wafer, and also on a second n+-GaAs acceptor wafer. The two wafers were then thermal compression bonded at the metallic interfaces. The substrate of the QCL wafer was lapped to 10 μm, and removed by selective wet-chemical etching. Following wet-etching of the laser ridges, Ti/Au (10/150 nm) was deposited on the top. The substrate was thinned and metallised to improve thermal performance, and the ridges were then cleaved and indium-soldered onto a copper submount.

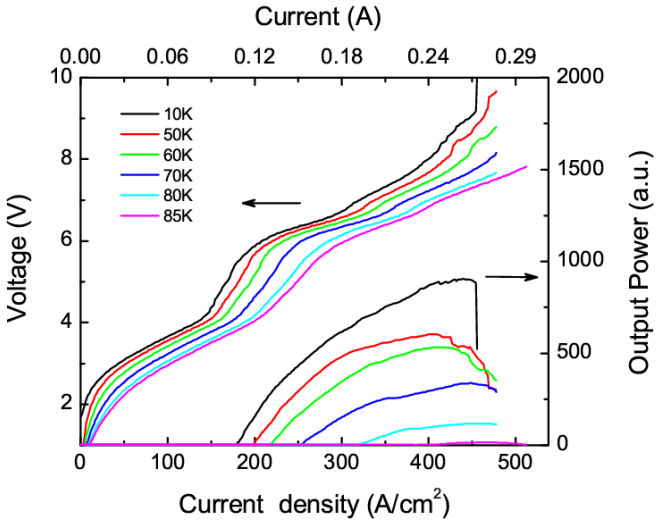

Figure 1. L–I–V curves at different temperatures. The device (980×60 μm^2) was operated in CW mode.

For the light intensity–current–voltage (L–I–V) characterization, the devices were mounted on the cold finger of a helium-cooled cryostat and operated in continuous wave (CW) mode. The laser emission was detected using a cooled Ge:Ga bolometer. Fig. 1 shows the L–I–V characteristics obtained at different temperatures. The maximum operating temperature is 85 K, at the temperature of 10 K, the dynamic range is from 179 A/cm^2 to 454 A/cm^2.

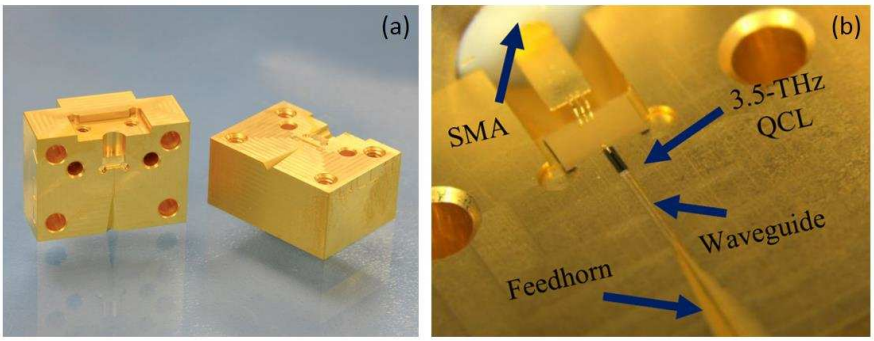

Figure 2. (a) Micromachined waveguide block assembly, (b) THz QCL mounted within a 150-μm-wide waveguide channel[25].

Compared with a semi-insulating surface-plasmon waveguide, DM waveguides yield lower threshold gain, leading to better continuous-wave (CW) performance and wider frequency tunability. However, the wider beam divergence and smaller aperture make optical alignment and feedback more difficult. In order to increase the reinjection efficiency of the optical feedback, a waveguide block with a diagonal feedhorn was micro-machined to couple radiation between the front facet and free space. A separate QCL device with the dimensions of 60 μm × 980 μm was processed as described above.

The substrate was reduced to 100 μm using mechanical lapping, and diced into a standalone 100-μm-wide chip. Fig. 2 (a) shows the micro-machined waveguide block assembly, including two half-blocks with a diagonal feedhorn, rectangular waveguide, mounting-point for an electrical SMA connector and the QCL-mounting recess. As shown in Fig. 2 (b), the QCL chip was solder-mounted within a precision micro-machined waveguide channel and ribbon-bonded to an integrated SMA connector. The other symmetrical half-block was attached above the QCL to form a rectangular waveguide (160 × 80 μm^2) enclosure around the device. The feedhorn and waveguide integrated device was shown to offer significantly improved performance over a non-integrated DM QCL[25].

3. EXPERIMENTAL SETUP

The optical configuration of the spectroscopy system is similar to that in Ref. 23, and is illustrated in Fig. 3. The emitted radiation from the QCL was directed through a 96.5-cm-long gas cell and was reflected back using a mechanically-adjustable optical delay-line into the QCL along the same optical path. The SM-perturbations to the QCL voltage were measured as a function of the optical delay time, and a Fast Fourier Transform (FFT) was used to infer the full-band emission spectrum of the QCL. The QCL operated in CW mode using an Arroyo 4320 current source and at a 10-K heatsink temperature within a Janis ST-100 He cooled cryostat. The gas cell has two polymethylpentene (TPX) windows mounted at 45° on each end, which is used to decrease etalon effects within the cell. A dry mechanical pump was used to evacuate the gas cell resulting in a base pressure of 0.03 Torr. A high-purity methanol sample was degassed and evaporated into the gas cell to the desired pressure measured by a capacitance manometer (MKS α-Baratron AA01).

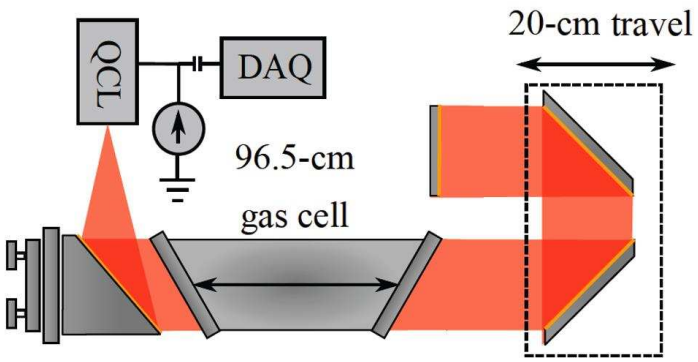

Figure 3. Schematic illustration of the configuration of the gas spectroscopy system[23].

The optical delay time was controlled using Newport ILS-200 motor translation stage, with a speed of 100 mm/s, and with measurements being triggered at 1-μm increments over a maximum distance of 200 mm. The perturbation of the QCL terminal voltage was recorded as a function of the displacement via a Stanford SR 560 preamplifier and a National Instruments USB-6216 data-acquisition board. With this setup, a spectrum can be obtained in 10 seconds. The maximum 800-mm round-trip delay (using beam-folding optics as in Fig. 3) corresponds to an FFT sampling resolution of around 380 MHz, and the 1-μm step size corresponds to an FFT spectral bandwidth of 37 THz.

Emission spectra of the QCL were measured at a temperature of 10 K, with dc driving currents sweeping at a range from 110 mA to 245 mA, and with the gas cell under vacuum. As shown in Fig. 4 (a), multi-mode emission was obtained with two main emission lines around 3.362 THz (mode A) and 3.428 THz (mode B) being observed simultaneously across the full dynamic range. Several lower-intensity side modes were also observed around the main emission lines over limited current ranges. Effective refractive indices of 4.046 and 4.036 were calculated for the side-modes around the 3.362 and 3.428 THz lines respectively, indicating that they originate from lateral confinement. To estimate the frequency evolution of the two main modes, the emission frequencies are plotted in Fig. 4 (b) and (c) as a function of current. The peak frequencies were obtained by using a Gaussian fit to the measured spectra. As the current was increased, both laser modes were shown to have a red shift with the frequency tuning ranges around 10 GHz in each case: from 3.3696–3.3594 THz and 3.4354–3.4253 THz, respectively. Both tuning curves can be divided into three piecewise-linear segments. This gives tuning rates of −380 MHz/mA, −173 MHz/mA and −31 MHz/mA for mode A, and −340 MHz/mA, −171 MHz/mA and −34 MHz/mA for mode B, respectively. The nonlinear frequency tuning characteristics can be attributed to a bias-induced gain shift and a thermal change in the refractive index.

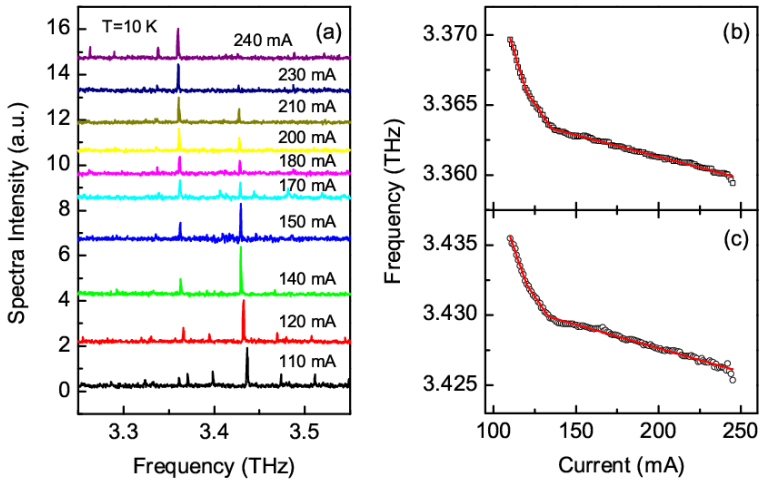

Figure 4. (a) Emission spectra of a THz QCL as a function of dc drive current, measured through self-mixing interferometry at 10 K and with the gas cell under vacuum. (b) and (c) The frequency of the two highest-intensity laser modes as a function of drive current. The red lines are three-segment linear fits to the experiment data (scatters)[26].

During the measurement, data were recorded with the translation stage moving in forward or reverse directions to reduce data-acquisition time, and 10 scans were averaged for every current step to decrease noise and remove SM hysteresis effects. A current-sweep step of 1.0 mA was used in Fig. 4 (b) and (c). As such, a data-acquisition rate of 0.05 samples/s was obtained, giving a total scan time of 2720 s to sweep the whole current range. The finest current step achievable using the DC source is 0.1 mA, corresponding to frequency tuning steps of 38 MHz, 17 MHz and 3 MHz for the three segments respectively. The frequencies in Fig. 4 exhibit small perturbations when the current is higher than 135 mA, due to SM frequency-pulling effects[23, 27]. The maximum frequency perturbation is less than 200 MHz, only half of the frequency resolution of the system. Thus, this frequency perturbation has weak influence on the measurement and is neglected during the data processing.

4. SELF-MIXING GAS SPECTROSCOPY

We assume that different laser modes operate independently in the Fabry-Pérot resonator of the QCL. Thus, the SM induced voltage modulation amplitude can be given by the sum of the contributions from all the individual laser modes[19, 23], using

$$U_{SM} \propto \sum_i T_i \cos\{\phi_{0i} - C_i \sin[\phi_i - \arctan(\alpha_i)]\}, \quad (1)$$

where i is the index of each laser mode, T_i is single-pass Beer–Lambert power transmission factor, ϕ_{0i} is the round-trip phase delay without optical feedback, C_i is the feedback strength, ϕ_i is the phase delay with optical feedback and α_i is the linewidth-enhancement factor. The phase delay can be expressed in terms of the laser mode frequency ν_{0i} and the external cavity round-trip time τ_i as

$$\phi_{0i} = 2\pi \nu_{0i} \tau_i. \quad (2)$$

In the case of weak feedback ($C \ll 1$), which can be justified by the long optical path-length in the system, the SM voltage modulation can be simplified to a closed analytical form,

$$U_{SM} \propto \sum_i T_i \cos(2\pi \nu_{0i} \tau_i). \quad (3)$$

Since the voltage modulation U_{SM} is dependent on the power transmission factors of all the laser modes, T_i, the integrated in situ frequency monitoring scheme is necessary for the identification of gas absorption features. In the frequency domain, Equation 3 becomes

$$U_{SM}(\nu) \propto \sum_i T_i \delta_{\nu,\nu_{0i}}. \quad (4)$$

As such, the laser mode intensity obtained from the SM interferogram is proportional to the corresponding power transmission factor. The transmission spectra of gases, therefore, can be measured by sweeping the mode frequencies of the QCL, with and without the gas present within the cell, and the gas absorption coefficient, α, can be calculated using the familiar Beer–Lambert law:

$$\alpha = -\ln(A/A_0)/L_{cell}, \tag{5}$$

where A and A_0 are the respective amplitudes of the transmission spectra with and without gas in the cell, and L_{cell} is the length of the gas cell. Note that the transmission spectra can be obtained simultaneously for all the laser modes by using this approach, which is much more efficient than SM spectroscopy based on single-mode lasers.

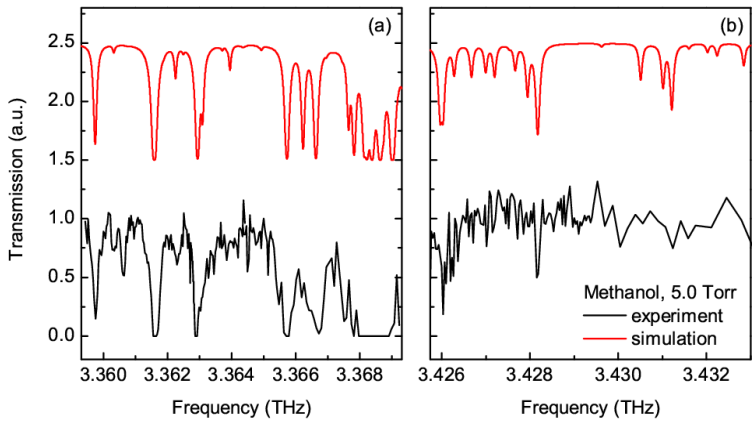

Figure 5. Transmission spectra of methanol at the pressure of 5.0 Torr, measured with (a) the laser mode A and (b) the laser mode B simultaneously[26]. The red lines are the calculated spectra based on data from the JPL molecular spectroscopy catalog[28], and the black lines are the measured results.

To demonstrate the validity of this approach, the emission frequency and intensity of the two laser modes were measured over the full dynamic current range with and without methanol vapor in the cell. Figure 5 shows the normalized transmission spectra of methanol at a pressure of 5.0 Torr. The use of a multi-mode QCL yielded a total measurement bandwidth of 17 GHz, much wider than the 2 GHz obtained using a single mode QCL[19, 23]. As such, eight absorption peaks and one absorption band were resolved. For comparison, the spectra were simulated based on data in the JPL molecular spectroscopy catalog[28], using a Voigt profile to account for self-broadening and Doppler broadening[23]. A small frequency offset between the measured and simulated spectra was observed, which could be attributed to a calibration offset in the motion controller. With a correction of −0.6 GHz (0.02%), the measured spectra agree well with the catalogued data. The absorption peaks of methanol and the respective rotational transitions are listed in Table 1.1, in which the peaks at 3.3597 THz, 3.3616 THz, 3.3629 THz, and 3.4282 THz are relatively well resolved. With lower pressure and a smaller current scanning step, more peaks could potentially be resolved within the broad absorption band around 3.3685 THz.

The minimum detectable absorption is an important performance metric for the spectrometer. It is dependent on the power of the laser source and the noise level of the system[14]. In our case, a multi-mode laser is used, and the different intensity of the laser modes will result in different minimum detectable absorption in each measurement band. This difference would also exist for one laser mode whose intensity varies across a wide frequency range. To assess the sensitivity of our SM approach, the minimum detectable absorption coefficient was calculated for the two main laser modes, using the standard deviation of the baseline transmission. The minimum detectable absorption coefficient is 2.7×10^{-4} cm^{-1} and 4.9×10^{-4} cm^{-1} for methanol at 3.3616 THz and 3.4282 THz respectively. The higher sensitivity at 3.3616 THz is due to the higher intensity of the corresponding laser mode. Compared with the minimum detectable coefficient of 1.0×10^{-4} cm^{-1} obtained with a surface plasmon QCL[23], the lower sensitivity of our measurement is mainly attributed to the lower optical feedback power of the double-metal device. Additionally, we note that there are small oscillations in the baseline of the transmission spectra, which also contribute to the higher minimum detectable absorption coefficient. This may be due to thermally-induced optical misalignment and frequency shift, and higher sensitivity can be expected by applying better thermal management.

Table 1. Key transitions of methanol, shown in figure 5, and their related rotational quantum levels. The data are from the JPL molecular spectroscopy catalog[28], where f is the frequency, J is the total angular momentum, K is the projection along the symmetry a-axis, vt is the torsional symmetry, INT is the base 10 logarithm of the integrated intensity.

f (THz)	upper state (J, K, v_t)	lower state (J, K, v_t)	INT ($nm^2 \cdot MHz$)
3.35973	22, 6, 1	22, 5, 1	-2.5622
3.36158	10, 9, 1	9, 8, 1	-2.0336
3.36293	15, a3, 0	14, a2, 0	-2.2010
3.36572	17, 14, 0	16, 13, 0	-2.2026
3.36622	21, 6, 1	21, 5, 1	-2.4921
3.36662	9, -5, 1	8, -4, 1	-2.2348
3.42603	22, -4, 2	23, +3, 1	-2.8940
3.42817	29, -7, 1; 29, 7, 1;	29, 6, 1; 29, -6, 1;	-2.9727 -2.9727

5. CONCLUSIONS

In summary, broadband THz gas spectroscopy has been demonstrated using self-mixing interferometry in a multimode double-metal THz QCL for the first time. The transmission spectra of methanol were simultaneously obtained within two distinct frequency ranges from 3.359 THz to 3.369 THz and from 3.426 THz to 3.433 THz. This approach has increased the total measurement bandwidth obtainable using a QCL-based SM scheme by a factor of ~7 and underpins future work to develop the first broadband “detector-free” multi-gas QCL spectroscopy systems.

FUNDING

UK Centre for Earth Observation Instrumentation (RP10G0435A03); European Space Agency (GSTP 4000114487/15/NL/AF); Royal Society (WM150029); Engineering and Physical Sciences Research Council (EPSRC) (EP/J017671/1, EP/P021859/1); European Research Council (ERC) (THEMIS 727541).

REFERENCES

[1] Siegel, P. H., "Terahertz technology," IEEE Trans. Microw. Theory 50, 910 (2002).
[2] Tonouchi, M., "Cutting-edge terahertz technology," Nature Photonics 1, 97 (2007).
[3] Baxter, J. B. and Guglietta, G. W., "Terahertz Spectroscopy," Anal. Chem. 83, 4342 (2011).
[4] Köhler, R., Tredicucci, A., Beltram, F., Beere, H. E., Linfield, E. H., Davies, A. G., Ritchie, D. A., Iotti, R. C. and Rossi, F., "Terahertz semiconductor-heterostructure laser," Nature 417, 156 (2002).
[5] Walther, C., Fischer, M., Scalari, G., Terazzi, R., Hoyler, N. and Faist, J., "Quantum cascade lasers operating from 1.2 to 1.6 THz," Appl. Phys. Lett. 91, 131122 (2007).
[6] Wienold, M., Röben, B., Lü, X., Rozas, G., Schrottke, L., Biermann, K. and Grahn, H. T., "Frequency dependence of the maximum operating temperature for quantum-cascade lasers up to 5.4 THz," Appl. Phys. Lett. 107, 202101 (2015).
[7] Barkan, A., Tittel, F. K., Mittleman, D. M., Dengler, R., Siegel, P. H., Scalari, G., Ajili, L., Faist, J., Beere, H. E., Linfield, E. H., Davies, A. G. and Ritchie, D. A., "Linewidth and tuning characteristics of terahertz quantum cascade lasers," Opt. Lett. 29, 575 (2004).

[8] Qin, Q., Reno, J. L. and Hu, Q., "MEMS-based tunable terahertz wire-laser over 330 GHz," Opt. Lett. 36, 692 (2011).
[9] Vitiello, M. S. and Tredicucci, A., "Tunable Emission in THz Quantum Cascade Lasers," IEEE Trans. Terahertz. Sci. Technol. 1, 76 (2011).
[10] Li, L. H., Chen, L., Freeman, J. R., Salih, M., Dean, P., Davies, A. G. and Linfield, E. H., "Multi-Watt high-power THz frequency quantum cascade lasers," Electron. Lett. 53, 799 (2017).
[11] Gao, J. R., Hovenier, J. N., Yang, Z. Q., Baselmans, J. J. A., Baryshev, A., Hajenius, M., Klapwijk, T. M., Adam, A. J. L., Klaassen, T. O., Williams, B. Kumar, S., S., Hu, Q. and Reno, J. L., "Terahertz heterodyne receiver based on a quantum cascade laser and a superconducting bolometer," Appl. Phys. Lett. 86, 244104 (2005).
[12] Richter, H., Semenov, A. D., Pavlov, S. G., Mahler, L., Tredicucci, A., Beere, H. E., Ritchie, D. A., Il'in, K. S., Siegel, M. and Hübers, H.-W., "Terahertz heterodyne receiver with quantum cascade laser and hot electron bolometer mixer in a pulse tube cooler," Appl. Phys. Lett. 93, 141108 (2008).
[13] Hübers, H.-W., Pavlov, S. G., Richter, H., Semenov, A. D., Mahler, L., Tredicucci, A., Beere, H. E. and Ritchie, D. A., "High-resolution gas phase spectroscopy with a distributed feedback terahertz quantum cascade laser". Appl. Phys. Lett. 89, 061115 (2006).
[14] Hübers, H.-W., Richter, H., Pavlov, S. G. and Richter, H., "High Resolution Terahertz Spectroscopy with Quantum Cascade Lasers," J. Infrared Millim. Terahertz Waves 34, 325 (2013).
[15] Ren, Y., Hayton, D. J., Hovenier, J. N., Cui, M., Gao, J. R., Klapwijk, T. M., Shi, S. C., Kao, T.-Y., Hu, Q. and Reno, J. L., "Frequency and amplitude stabilized terahertz quantum cascade laser as local oscillator," Appl. Phys. Lett. 101, 101111 (2012).
[16] Eichholz, R., Richter, H,. Wienold, M., Schrottke, L., Hey, R., Grahn, H. T. and Hübers, H.-W., "Frequency modulation spectroscopy with a THz quantum-cascade laser," Opt. Express 21, 32199 (2013).
[17] Hangauer, A., Westberg, Zhang, J., E. and Wysocki, G., "Wavelength modulated multiheterodyne spectroscopy using Fabry-Pérot quantum cascade lasers," Opt. Express, 24, 25298 (2016).
[18] Patimisco, P., Borri, S., Sampaolo, A., Beere, H. E., Ritchie, D. A., Vitiello, M. S., Scamarcio, G. and Spagnolo, V., "A quartz enhanced photo-acoustic gas sensor based on a custom tuning fork and a terahertz quantum cascade laser," Analyst 139, 2079 (2004).
[19] Hagelschuer, T., Wienold, M., Richter, H., Schrottke, L., Biermann, K., Grahn, H. T. and Hübers, H.-W., "Terahertz gas spectroscopy through self-mixing in a quantum-cascade laser," Appl. Phys. Lett. 109, 191101 (2016).
[20] Lang R. and Kobayashi, K., "External optical feedback effects on semiconductor injection laser properties," IEEE J. Quantum Electron. 16, 347 (1980).
[21] Taimre, T., Nikolić, M., Bertling, K., Lim, Y. L., Bosch, T. and Rakić, A. D., "Laser feedback interferometry: a tutorial on the self-mixing effect for coherent sensing," Adv. Opt. Photon. 7, 570 (2015).
[22] Hagelschuer, T., Wienold, M., Richter, H., Schrottke, L., Grahn, H. T. and Hübers, H.-W., "Real-time gas sensing based on optical feedback in a terahertz quantum-cascade laser," Opt. Express 25, 30203 (2017).
[23] Chhantyal-Pun, R., Valavanis, A., Keeley, J., Rubino, P., Kundu, I., Han, Y. J., Dean, P., Li, L. H., Davies, A. G. and Linfield, E. H., "Gas spectroscopy with integrated frequency monitoring through self-mixing in a terahertz quantum-cascade laser," Opt. Lett. 43, 2225 (2018).
[24] Han, Y. J., Li, L. H., Valavanis, A., Brewster, N., Zhu, J. X., Dong, R., Dean, P., Bushnell, L., Oldfield, M., Davies, A. G., Ellison, B. N. and Linfield, E. H., "Development of terahertz frequency quantum cascade lasers for the applications as local oscillators," THz for CBRN and Explosives Detection and Diagnosis, 123 (2017).
[25] Valavanis, A., Henry, M., Han, Y., Auriacombe, O., Dong, R., Rawlings, T., Li, L. H., Oldfield, M., Brewster, N., Davies, A. G., Ellison, B. N. and Linfield, E. H., "Feedhorn-integrated THz QCL local oscillators for the LOCUS atmospheric sounder," IRMMW-THz, (2016).
[26] Han, Y. J., Partington, J., Valavanis, A., Chhantyal-Pun, R., Henry, Auriacombe, M., O., Rawlings, T., Li, L. H., Keeley, J., Oldfield, M., Brewster, N., Dong, R., Dean, P., Davies, A. G., Ellison, B. N. and Linfield, E. H., "Gas spectroscopy through multimode self-mixing in a double-metal terahertz quantum cascade laser," IQCLSW, (2018).
[27] Keeley, J., Freeman, J., Bertling, K., Lim, Y. L., Mohandas, R. A., Taimre, T., Li, L. H., Indjin, D., Rakić, A. D., Linfield, E. H., Davies, A. G. and Dean., P., "Measurement of the emission spectrum of a semiconductor laser using laser-feedback interferometry," Sci. Rep. 7, 7236 (2017).

[28] Pickett, H. M., Poynter, R. L., Cohen, E. A., Delitsky, M. L., Pearson, J. C. and P. Müller, H. S., "Submillimeter, millimeter, and microwave spectral line catalog," J. Quant. Spectrosc. Radiat. Transfer 60, 883 (1998).